STEM CELLS TRANSLATIONAL MEDICINE®

ENABLING TECHNOLOGIES FOR CELL-BASED CLINICAL TRANSLATION

Fluorine-19 Labeling of Stromal Vascular Fraction Cells for Clinical Imaging Applications

LAURA C. ROSE,[a,b] DEEPAK K. KADAYAKKARA,[a,b,c] GUAN WANG,[d] AMNON BAR-SHIR,[a,b] BROOKE M. HELFER,[e] CHARLES F. O'HANLON,[e] DARA L. KRAITCHMAN,[a,f] RICARDO L. RODRIGUEZ,[g] JEFF W.M. BULTE[a,b,c,h,i]

Key Words. Stromal vascular fraction • Liposuction • Magnetic resonance imaging • Fluorine • Cell tracking • Breast cancer • Radiation-induced fibrosis

[a]Division of Magnetic Resonance Research, Russell H. Morgan Department of Radiology and Radiological Science, [b]Cellular Imaging Section and Vascular Biology Program, Institute for Cell Engineering, [c]Department of Oncology, [d]Department of Electrical and Computer Engineering, [f]Department of Molecular and Comparative Pathobiology, [h]Department of Biomedical Engineering, and [i]Department of Chemical & Biomolecular Engineering, The Johns Hopkins University School of Medicine, Baltimore, Maryland, USA; [e]Celsense Inc., Pittsburgh, Pennsylvania, USA; [g]CosmeticSurg, LLC, Luthersville, Maryland, USA

Correspondence: Jeff W.M. Bulte, Ph.D., Russell H. Morgan Department of Radiology and Radiological Science, Division of Magnetic Resonance Research, The Johns Hopkins University School of Medicine, 217 Traylor Building, 720 Rutland Avenue, Baltimore, Maryland 21205, USA. E-Mail: jwmbulte@mri.jhu.edu

Received May 26, 2015; accepted for publication August 31, 2015; published Online First on October 28, 2015.

1066-5099/2015/$20.00/0

http://dx.doi.org/10.5966/sctm.2015-0113

ABSTRACT

Stromal vascular fraction (SVF) cells are used clinically for various therapeutic targets. The location and persistence of engrafted SVF cells are important parameters for determining treatment failure versus success. We used the GID SVF-1 platform and a clinical protocol to harvest and label SVF cells with the fluorinated (^{19}F) agent CS-1000 as part of a first-in-human phase I trial (clinicaltrials.gov identifier NCT02035085) to track SVF cells with magnetic resonance imaging during treatment of radiation-induced fibrosis in breast cancer patients. Flow cytometry revealed that SVF cells consisted of 25.0% ± 15.8% CD45+, 24.6% ± 12.5% CD34+, and 7.5% ± 3.3% CD31+ cells, with 2.1 ± 0.7 × 10^5 cells per cubic centimeter of adipose tissue obtained. Fluorescent CS-1000 (CS-ATM DM Green) labeled 87.0% ± 13.5% of CD34+ progenitor cells compared with 47.8% ± 18.5% of hematopoietic CD45+ cells, with an average of 2.8 ± 2.0 × 10^{12} ^{19}F atoms per cell, determined using nuclear magnetic resonance spectroscopy. The vast majority (92.7% ± 5.0%) of CD31+ cells were also labeled, although most coexpressed CD34. Only 16% ± 22.3% of CD45−/CD31−/CD34− (triple-negative) cells were labeled with CS-ATM DM Green. After induction of cell death by either apoptosis or necrosis, >95% of ^{19}F was released from the cells, indicating that fluorine retention can be used as a surrogate marker for cell survival. Labeled-SVF cells engrafted in a silicone breast phantom could be visualized with a clinical 3-Tesla magnetic resonance imaging scanner at a sensitivity of approximately 2 × 10^6 cells at a depth of 5 mm. The current protocol can be used to image transplanted SVF cells at clinically relevant cell concentrations in patients. STEM CELLS TRANSLATIONAL MEDICINE *2015;4:1472–1481*

SIGNIFICANCE

Stromal vascular fraction (SVF) cells harvested from adipose tissue offer great promise in regenerative medicine, but methods to track such cell therapies are needed to ensure correct administration and monitor survival. A clinical protocol was developed to harvest and label SVF cells with the fluorinated (^{19}F) agent CS-1000, allowing cells to be tracked with ^{19}F magnetic resonance imaging (MRI). Flow cytometry evaluation revealed heterogeneous ^{19}F uptake in SVF cells, confirming the need for careful characterization. The proposed protocol resulted in sufficient ^{19}F uptake to allow imaging using a clinical MRI scanner with point-of-care processing.

INTRODUCTION

Approximately 100,000 women in the United States undergo breast lumpectomy and irradiation every year. Of these women, 10%–30% can develop late painful or disabling complications from radiotherapy. Radiation damage to the soft tissues is referred to as radiation-induced fibrosis (RIF) and is considered irreversible [1–3]. Grafting of autologous fat tissue, obtained by liposuction, for treatment of RIF of the breast is now a common procedure, reimbursed by most insurance companies. For further refinement of fat grafting using stem cells as a supplement, a preference toward using stromal vascular fraction (SVF) cells appears to be increasing, as shown by Gentile et al. [4], who obtained a 63%–69% maintenance of breast contour-restoring and three-dimensional volume using SVF-purified cells, compared with 39% maintenance using centrifuged fat grafting only [5]. The initial rationale for using SVF cells or the nonadipocyte fraction of adipose tissue as a supplement to adipose tissue grafting was to increase the efficiency of the fat grafting [6], with the salutary effects on the treatment of RIF using SVF cells an unexpected finding in the studies by Rigotti et al. [7]. SVF-enhanced fat grafting has also been used for other forms of breast reconstructive surgery,

including augmentation [8], postmastectomy reconstruction [9], and breast implant complications [10].

The fate of SVF cells after engraftment is at present difficult to address. Owing to inconsistencies in the outcome of previous cell therapies [11], along with the uncertain accuracy of administering cells into the target tissue [12], noninvasive clinical imaging techniques that could visualize the initial location of cell deposits, the potential migration away from the grafting site, and the duration of overall cell survival would be extremely valuable for the further development of SVF cell therapy. Radionuclide imaging using ^{111}In-oxine [13, 14] and ^{1}H-based magnetic resonance imaging (MRI) using superparamagnetic iron oxide (SPIO) particles [15] have previously been used to track stem and progenitor cells in patients in vivo. The manufacture of the clinical grade SPIO used in MRI cell tracking studies was discontinued in 2008 for economic reasons [15], leading current preclinical studies to resort to "off-label" use of Food and Drug Administration (FDA)-approved iron supplements to track cells [16–18]. SPIO-loaded cells cause signal loss on T_2-weighted MRI. However, detection has been hampered by the existence of similar characteristic hypointense regions from other sources, including tissue damage and hemorrhage, making this labeling method impractical for our purposes. The surgical act of introducing the cells directly into RIF tissue itself could cause tissue damage and hemorrhage, thus filling the area with artifacts. In contrast, radioactive tracers allow a clear detection of transplanted cells as "hot spots," because no background signal is present. Radiolabels, however, are limited to cell tracking for short periods of time (days) and need additional imaging modalities for anatomical localization.

Fluorine-19 (^{19}F) MRI is a relatively newer cell tracking technique [19–22] that also allows "hot spot" detection [23], owing to the absence of fluorine in the human body, except for the immobilized trace amounts bound to the teeth. Importantly, the anatomical location of the engraftment can be determined by overlaying ^{19}F MRI with conventional ^{1}H MRI, only requiring retuning of the nuclear magnetic resonance (NMR) frequency using a multinuclear coil. As a part of an investigational new drug (IND) submission for the treatment of RIF in breast cancer patients (ClinicalTrials.gov identifier NCT02035085), we present a protocol for labeling SVF cells with CS-1000, a perfluorocarbon (PFC) and ^{19}F-rich agent that recently received IND approval for imaging colorectal cancer vaccines [24].

No studies have been performed on SVF-PFC labeling, and few studies have been performed on the uptake of other labels in SVF cells. Despite the heterogeneity of SVF cells, none of the previous non-PFC-labeling studies investigated which SVF subpopulations took up the label [14, 25] or at what percentage. Because of the increasing use of SVF cells in clinical treatment and recent efforts to develop fluorine MRI cell tracking, we undertook a detailed study of PFC labeling of SVF subpopulations with CS-1000. We developed a same-day SVF harvesting and labeling clinical protocol (point-of-care processing) to obtain a cell product that does not require cell culture, circumventing the regulatory hurdles associated with cultured cell products, and determined the sensitivity of cell detection using a clinical imaging setup.

Materials and Methods

Materials

The GID SVF-1 device was provided by the GID Group (Louisville, CO, http://www.thegidgroup.com). Lactated Ringer's solution was obtained from Hospira (Lake Forest, IL, http://www.hospira.com). Histopaque-1077, trifluoroacetic acid (TFA), staurosporine, deuterium oxide, agarose, and 4′,6-diamidino-2-phenylindole dihydrochloride (DAPI) were purchased from Sigma-Aldrich (St. Louis, MO, http://www.sigmaaldrich.com). Dulbecco's modified Eagle's medium (DMEM), Hank's balanced salt solution (HBSS), ammonium-chloride-potassium (ACK) lysing buffer, trypan blue, and Triton X-100 was purchased from Life Technologies (Grand Island, NY, http://www.lifetechnologies.com). Phosphate-buffered saline (PBS) was purchased from Corning (Manassas, VA, http://www.corning.com). Celsense Inc. (Pittsburgh, PA, http://www.celsense.com) provided CS-1000 and dual mode CS-ATM DM Green for these studies. Bovine serum albumin (BSA) was purchased from Amresco (Solon, OH, http://www.amresco-inc.com). Antibodies against CD13, CD34, and CD45 and their isotype controls were purchased from BioLegend (San Diego, CA, http://www.biolegend.com). Tryptic soy broth (TSB) was purchased from Millipore (Billerica, MA, http://www.emdmillipore.com).

SVF Harvesting and Processing

Our institutional review board approved all protocols involving human subjects. Adipose tissue was harvested from the flanks of healthy female patients (age, 20–47 years) undergoing liposuction of the abdominal area. The adipose tissue for harvesting was injected with tumescent solution consisting of 30 ml of 0.5% Marcaine with epinephrine 1:200,000 and 45 ml of 1% lidocaine with epinephrine 1:100,000 diluted in 3,000 ml of lactated Ringer's solution (LR). After a 20-minute period to allow for the full vasoconstriction and anesthetic effect, liposuction was performed using a 3-mm Sattler type cannula with 1-mm ostia at a pressure of −400 mmHg. The GID SVF-1 cell-harvesting platform was used to extract SVF cells from the adipose tissue [26]. The manufacturer's protocol using LR was modified to use 10 mM PBS (pH 7.4) without calcium and magnesium, for the reasons described in Results. In brief, fat was collected in the GID SVF-1 device with either LR or PBS containing 5,000 U.S. Pharmaceutical units per liter of heparin. After the last washing, the device was weighed to determine the total adipose tissue mass. For digestion, the fat was suspended in LR or PBS, to which a proprietary collagenase mix (GIDzyme suspended in LR) was added. LR or PBS and the GIDzyme addition was adjusted to the amount of fat collected, with 1 vial for 100–175 g of fat, 1.5 vials for 200–250 g, and 2 vials for 275–350 g. The device was incubated at 37°C for 40 minutes (LR and PBS) or 60 minutes (PBS only) on a shaking rocker. The collagenase reaction was stopped with BSA at a final concentration of 2.5%. Human serum albumin (HSA) has been proposed for clinical studies; however, owing to the expense of HSA and the large quantities required, BSA was used for our studies. The entire device was centrifuged for 10 minutes at 800*g* and the oil layer removed. Using the manufacturer's protocol, the pellet was resuspended in LR for further use.

For the modified protocol, additional washes were performed after removal of the oil layer. After a second centrifugation, the remaining supernatant was removed and the pellet transferred to a 50-ml conical tube for two additional washes with PBS. The SVF cells were treated with either ACK lysis buffer or density gradient centrifugation. In brief, the cells were either layered onto Histopaque and centrifuged for 30 minutes or incubated in a diluted ACK lysis buffer for 2–3 minutes at room temperature before being washed twice with PBS plus 0.5% BSA and resuspended in DMEM plus 0.5% BSA.

CS-1000 Labeling

Cell viability in DMEM plus 0.5% BSA was determined with trypan blue, and the cell concentration was adjusted to 1–5 million cells per milliliter for labeling. The cells were incubated with either CS-1000 or CS-ATM DM Green, a version of CS-1000 conjugated to a green fluorescent probe. For the initial ^{19}F-uptake studies, cells in DMEM plus 0.5% BSA were labeled with 2.5, 5, 10, or 20 mg/ml for 2 or 4 hours at 37°C with gentle shaking. Based on the results from these pilot studies, all further experiments were performed on cells labeled with 20 mg/ml CS-1000 for 4 hours. The cells were then washed three times and further analyzed as described. For cell death assays, the SVF cells were first allowed to adhere in tissue culture flasks under standard conditions of 37°C and 5% CO_2 in basic medium containing 10% fetal bovine serum and 1% penicillin/streptomycin. At the second passage, the cells were labeled for 24 hours with 10 mg/ml CS-1000 in DMEM without any additives. After three washes with PBS, the cells were returned to basic medium, basic medium with 1 μM staurosporine, or subjected to three freeze/thaw cycles at −20°C before being returned to the incubator. Four days later, the supernatant and adherent cells were collected. Floating or dead cells and cell fragments in the supernatant were collected by a 5-minute 800*g* centrifugation step and added back to the cell pellet. Cells were collected for NMR analysis of ^{19}F content. Replicates from three independent runs were pooled to obtain sufficient NMR signal.

Process Simulation

Our cell product is not subject to any form of sterilization and must therefore be harvested under aseptic conditions. To demonstrate that cells were aseptically harvested and labeled, we performed a process simulation, which is routinely used to demonstrate to regulatory agencies that a product can be manufactured aseptically. In such process simulations, microbial growth media, such as TSB, is run through the proposed protocol and then incubated to allow growth and detection of any microorganisms. Thus, the entire SVF harvest and CS-1000-labeling procedure was repeated with TSB instead of lipoaspirate. Throughout the entire process, samples were obtained at each step. After completion, all used containers and disposables with media, including the GID SVF-1 device and conical tubes for labeling, were also collected. The samples were incubated at 30°C for at least 14 days and monitored for changes in turbidity, which would indicate microbial growth.

Flow Cytometry and NMR Spectrometry

CS-1000-labeled cells were resuspended in PBS plus 0.5% BSA and incubated on ice with antibodies against CD31, CD34, and CD45 for 30 minutes. Single-color and isotype controls were also included. After antibody incubation, DAPI was added to the cells as a viability marker, and the cells were analyzed use a Becton-Dickinson LSR II flow cytometer (BD Biosciences, San Diego, CA, http://www.bdbiosciences.com). Live cells were gated from analysis by side/forward scatter and DAPI. Statistical significance was evaluated using a *t* test to compare the treatment groups. To determine the ^{19}F content, the samples were mixed with deuterium oxide containing Triton X-100, and each sample was spiked with 125 μl of 0.1% TFA as an internal reference. ^{19}F NMR spectra were acquired for each sample using a Bruker Avance 11.7 T (470 MHz) NMR spectrometer (Bruker Avance, Billerica, MA, http://www.bruker.com). The major CS-1000 peak at −91.5 ppm and TFA peak at −76 ppm were integrated. The ^{19}F content per sample was calculated as described in the following formula, where $I_{CS\text{-}1000}$ and I_{TFA} are the integrations of the ^{19}F signal in the ^{19}F NMR spectrum obtained from the CS-1000 sample and TFA peak, respectively, M_{TFA} is the number of moles of TFA in each sample, and $N_{Avogadro}$ is Avogadro's number.

$$^{19}\mathbf{F\ per\ sample} = \frac{3 \times \mathbf{I_{CS-1000}} \times \mathbf{M_{TFA}} \times \mathbf{N_{Avogadro}}}{\mathbf{I_{TFA}}}$$

To determine the total amount of ^{19}F atoms per cell, the calculated number per sample of atoms were normalized to the number of live cells in the sample.

^{1}H and ^{19}F MRI

Labeled cells were scanned on a Siemens TIM Trio 3 Tesla (T) MRI scanner. SVF cells (0.5–2 × 10^6 in 1 ml of PBS) cells were injected in a 350-ml Mentor silicone breast implant phantom, with CS-1000 standards of 1.0 and 2.0 mg/ml placed in agarose around the phantom. ^{1}H images were obtained using a six-channel, phased-array body matrix coil with a gradient echo sequence. The additional scan parameters were an echo time/repetition time (TE/TR) of 3.69 ms/15 ms, a field of view (FOV) of 325 × 400 mm, an image matrix of 64 × 416 × 512, a voxel size of 1.5 × 0.78 × 0.78 mm, and a 20° flip angle. ^{19}F images were obtained with a True Fast Imaging With Steady-State Precession (FISP) sequence using a custom-built, four-channel, phased-array surface coil. The scan parameters were a TE/TR of 1.6 ms/3.2 ms, FOV of 421 × 500 mm, matrix of 20 × 54 × 64, 32 signal averages, voxel size of 5.0 × 7.8 × 7.8 mm, 69° flip angle, 1-kHz bandwidth, and 3.5-minute acquisition time.

Results

SVF Harvesting

In the initial studies using the GID SVF-1 manufacturing protocol, the SVF was washed and enzymatically digested in LR. After the addition of serum to stop the reaction and centrifugation step, the SVF cells were diluted in LR for a 2–5-hour incubation to mimic CS-1000 labeling. A comparison of the labeling buffer revealed increased cell death with LR compared with the more commonly used preclinical buffers PBS and HBSS (Fig. 1A). After a 2-hour incubation, 55.9% of the cells in LR were dead, identified using DAPI viability staining, compared with 7.17% and 6.41% in PBS and HBSS, respectively. A similar pattern of increased cell death in LR was observed for a longer 5-hour incubation with similar samples from the same patient harvested in parallel with either LR or PBS (data not shown). Because of the consistently higher number of dead cells observed with LR, PBS was used for the subsequent harvests. One possible reason might have been that the presence of Ca^{2+} ions in LR binds to cadherins, causing reaggregation of cells after enzymatic digestion. Cadherins were discovered [27] after the observation that single cells prepared by trypsin digestion were reclumping when ethylenediaminetetraacetic acid, a metal chelate that binds calcium, was not present in the solution.

The manufacturer's protocol was further modified to address the turbidity of the supernatant of the cell pellet before resuspension and the large number of red blood cells (RBCs) in the cell pellet (Fig. 1B). After a single wash, the turbidity of the supernatant was so high that the label on the opposite side of the conical tube was completely obscured (Fig. 1Bi). An additional wash cleared the supernatant sufficiently to see the label

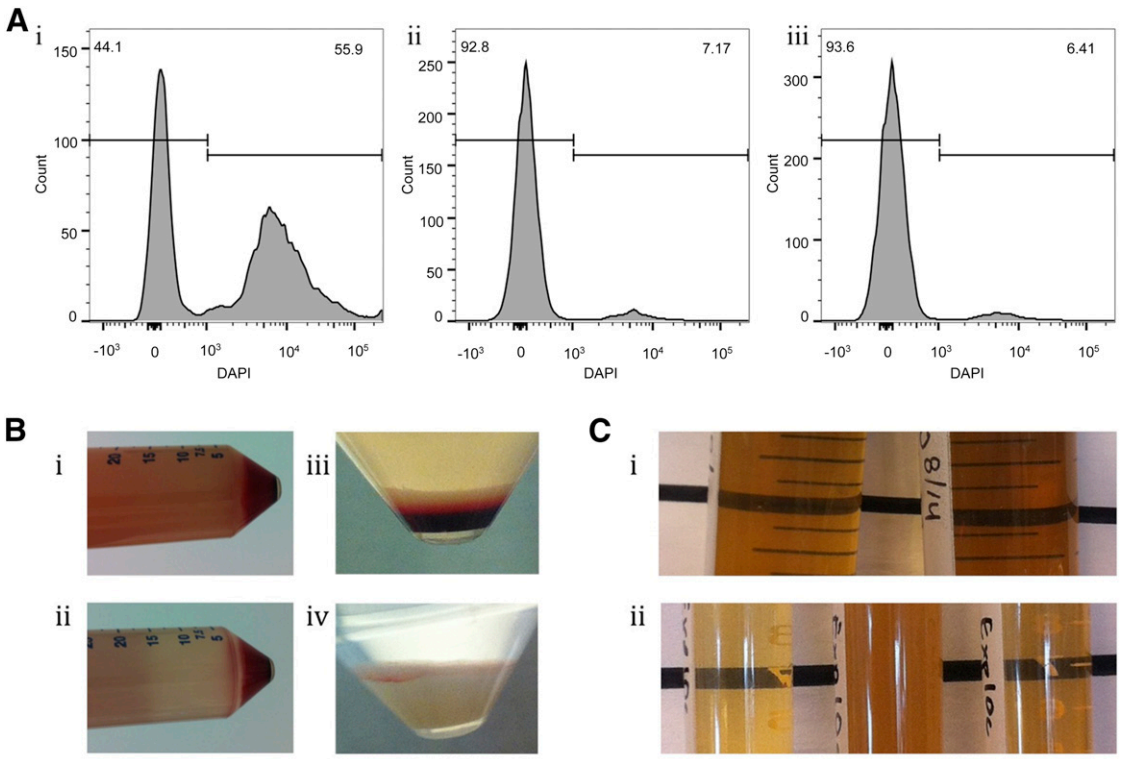

Figure 1. Development of clinical stromal vascular fraction (SVF) harvest protocol. Flow cytometry histograms show DAPI staining, with DAPI-positive cells gated **(A)**. The cells were incubated in lactated Ringer's solution **(Ai)**, phosphate-buffered saline (PBS) **(Aii)**, or Hank's balanced salt solution (HBSS) **(Aiii)** for 2 hours. SVF cell pellets were transferred from GID SVF-1 to conical tubes after one **(Bi)** or two **(Bii)** washes, and before **(Biii)** and after **(Biv)** red blood cell removal. Samples of tryptic soy broth (TSB) from process simulation **(Ci)** and standards (**[Cii]** left, negative control; middle, positive control; right, negative control) were incubated to determine bacterial contamination. Note the cloudiness of TSB only in the positive control. Abbreviation: DAPI, 4′,6-diamidino-2-phenylindole dihydrochloride.

on the opposite side of the tube (Fig. 1Bii). The large number of RBCs in the cell pellet necessitated a removal method (Fig. 1Biii), and both ACK lysis buffer and gradient centrifugation efficiently removed the RBCs. Additional washes in the RBC removal protocol cleared the supernatant of extracellular matrix, platelets, cell fragments, and other debris (Fig. 1Biv). Based on these findings, the protocol was modified to include sufficient washings and an RBC removal step.

To evaluate whether this protocol could produce a sterile final product, necessary for regulatory approval and clinical use, process simulation was conducted in which the bacteriological medium TSB was run through the entire protocol in place of tissue or cells (Fig. 1C). For the first process simulation, aliquots of TSB were removed throughout the protocol such that in the event of contamination, the time of microbial exposure could be identified. In addition to the samples, the containers for harvest and labeling, such as GID SVF-1 and conical tubes, were kept for incubation. After a clean run without any indication of growth, only the containers were incubated. After at least 14 days of incubation, no sign of microbial growth was noted in any of the process simulation samples (Fig. 1Ci) except for the positive controls exposed to a nonsterile environment (Fig. 1Cii). These results indicate that a sterile cell product can be obtained using the current protocol.

SVF Labeling

Pilot labeling studies investigating ^{19}F uptake in SVF cells demonstrated a dose- and time-dependent increase in ^{19}F uptake. An increase of 5–10 mg/ml led to a 2.4-fold increase in ^{19}F content, and an increase from 1 hour to 3 hours of incubation led to a 1.5-fold increase. Based on these studies, we used a concentration of 20 mg/ml and a 4-hour incubation period for additional studies. Dual-mode CS-ATM DM Green contains a green fluorescent probe detectable with flow cytometry and microscopy. With untreated cells set to 1% FL1-positive, CS-ATM DM Green-treated cells showed an increase in the FL1 channel compared with unlabeled cells (Fig. 2A). Comparable labeling was observed when cells were incubated in either PBS or DMEM; however, increased DAPI-positive dead cells were observed with PBS (Fig. 2B). No difference in the number of dead cells was observed between the labeled and unlabeled cells. Based on these findings, cells were incubated in DMEM for further analysis. To investigate how RBC removal treatments affected CS-1000 labeling, CS-1000 labeling was compared in the cells treated with either ACK lysis buffer or gradient centrifugation. Similar CS-1000 labeling efficiencies were observed for the samples treated with lysis buffer and centrifugation (Fig. 2C). With similar labeling efficiencies, ACK lysis was selected for all subsequent harvests. Flow cytometry was confirmed with fluorescence microscopy, in which cells labeled with CS-ATM DM Green were clearly observed (Fig. 2D).

SVF Cell Subset Analysis

The final SVF cell product was analyzed for CD45-positive hematopoietic lineage cells, CD31-positive endothelial lineage cells, and CD34-positive progenitor or stem cells using flow cytometry from four independent patient runs (Table 1). The total average yield was $2.13 \pm 0.7 \times 10^5$ total SVF cells per cubic centimeter of

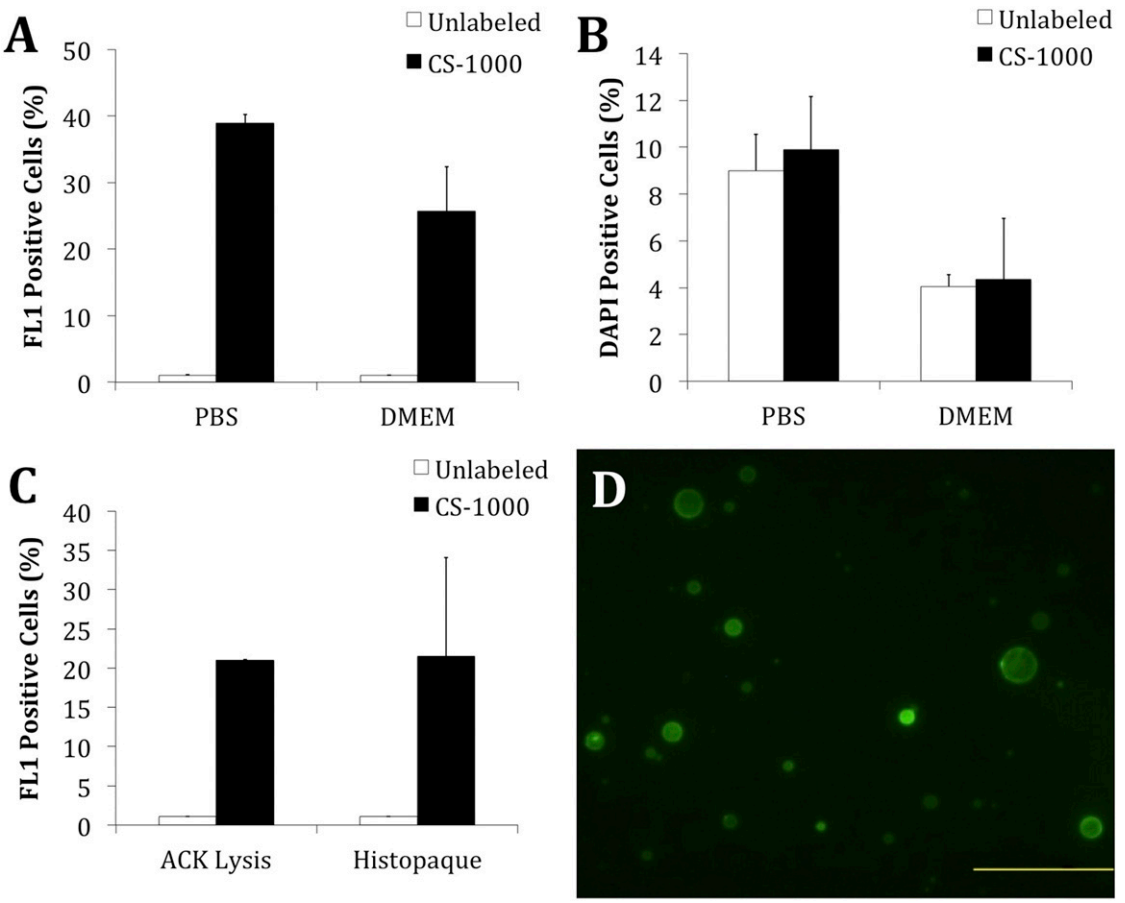

Figure 2. Development of clinical stromal vascular fraction (SVF) labeling protocol. **(A):** SVF cells were labeled with 20 mg/ml CS-ATM DM Green for 4 hours in either the PBS or the DMEM and analyzed with flow cytometry after ammonium-chloride-potassium (ACK) treatment. **(B):** Percentage of 4′,6-diamidino-2-phenylindole dihydrochloride-positive (viable) cells for the same PBS and DMEM groups shown in **(A)**. **(C):** To ensure that the choice of red blood cell (RBC) removal method did not affect ^{19}F labeling, SVF cells were treated with either ACK lysis buffer or gradient centrifugation to remove RBCs. The SVF cells were then labeled in DMEM with 20 mg/ml CS-ATM DM Green for 4 hours and analyzed with flow cytometry. **(D):** Labeling was confirmed with fluorescent microscopy (scale bar = 100 μm). Abbreviations: DMEM, Dulbecco's modified Eagle's medium; PBS, phosphate-buffered saline.

adipose tissue. Nearly equal proportions of CD45$^+$ hematopoietic and CD34$^+$ progenitor cells were observed at 25.0% and 24.6%, respectively. Of the total SVF cells, 3.98% expressed both CD45 and CD34, indicating that 15.9% of the hematopoietic lineage cells were progenitors. In contrast, 7.49% of all the cells were CD31-positive, with 7.20% expressing both CD31 and CD34, indicating that 96.0% of endothelial linage cells were progenitors. The percentage of remaining cells not expressing CD45, CD31, or CD34 was 55.2%.

To determine the CS-1000 uptake in these SVF subpopulations, the cells were incubated with CS-ATM DM Green and then stained with antibodies against CD45, CD31, and CD34 for flow cytometry analysis (Fig. 3; Table 2). CS-ATM DM Green labeled 37% of the total SVF cells, including CD45-, CD31-, and CD34-positive cells. Most CD34- and CD31-positive cells took up label, with labeling rates of 87.0% and 92.7%, respectively. Only 47.8% of the CD45-positive cells were labeled with CS-ATM DM Green, and a distinct group of unlabeled cells was observed. Of the remaining cells without any of the queried CD45, CD31, or CD34 markers, an average of 18% of cells were labeled.

^{19}F Labeling and Retention After Cell Death

The overall ^{19}F content as measured with NMR spectroscopy was $2.8 \pm 2.0 \times 10^{12}$ atoms per cell for the total SVF isolate. To investigate the fate of CS-1000 after apoptosis and necrosis, the labeled cells were exposed to staurosporine or freeze/thaw cycles, respectively, both of which resulted in widespread cell death. The culture medium was separated, and the adherent cells were trypsinized. From the culture medium, detached cells and cell debris were collected by centrifugation and added back to the trypsinized cell pellet to differentiate between CS-1000 remaining bound to cell fragments and CS-1000 released into the surrounding medium on cell death. ^{19}F NMR analysis of cells without cell death induction showed 90.6% of the fluorine was

Table 1. Characterization of final (unlabeled) stromal vascular fraction cell product

Marker-positive cells	Average ± SD, %
CD45+	25.0 ± 15.8
CD34+	24.6 ± 12.5
CD31+	7.5 ± 3.3
CD45+/CD34+	4.0 ± 3.5
CD31+/CD34+	7.2 ± 4.4
CD45−/CD31−/CD34−	55.2 ± 23.4

Data are presented for n = 4 independent experiments.

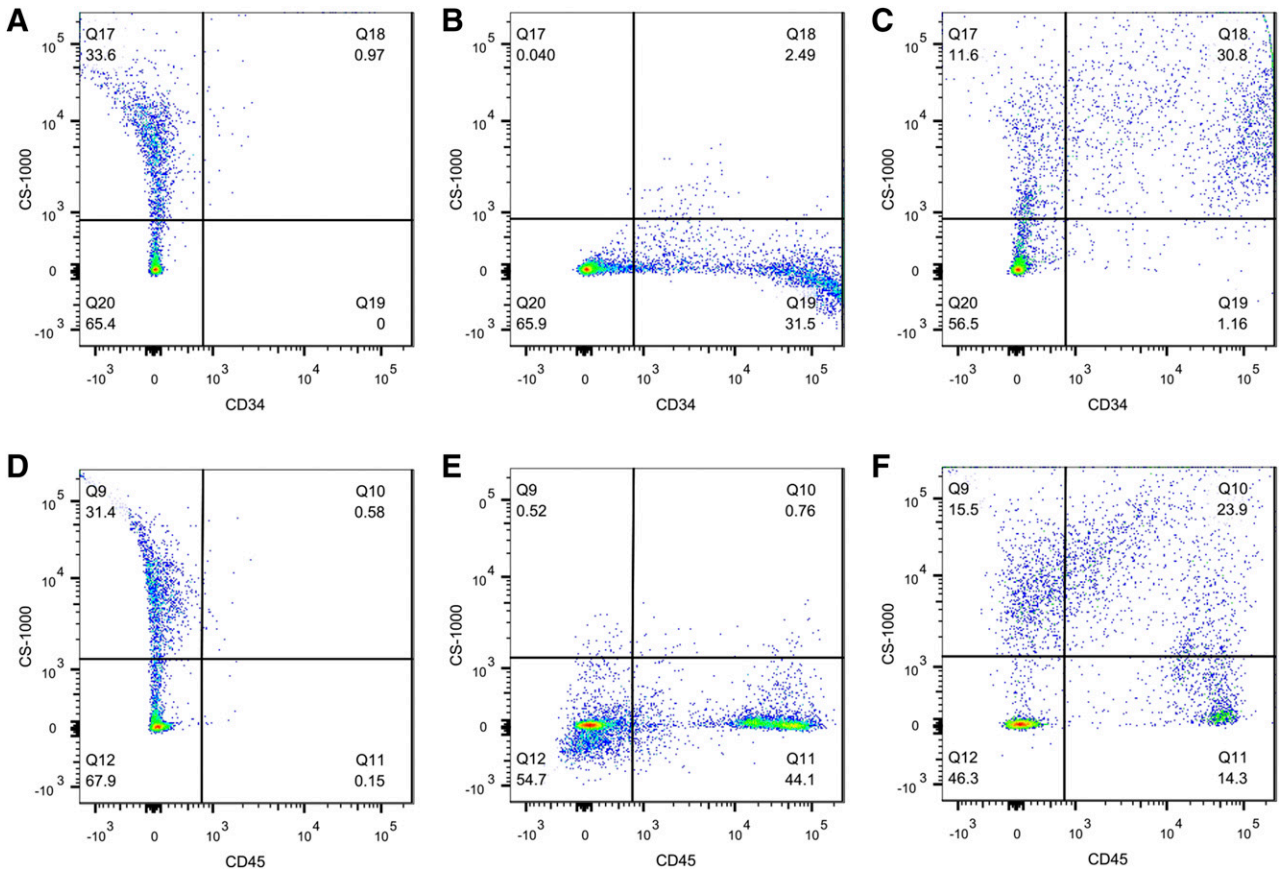

Figure 3. Stromal vascular fraction (SVF) cells labeled with CS-ATM DM Green. SVF cells labeled with dual mode CS-ATM DM Green (fluorescein isothiocyanate channel) were stained with anti-CD45 (allophycocyanin channel) and anti-CD34 (phycoerythrin channel) antibodies. Representative flow cytometry images show unstained CS-ATM DM Green-labeled cells **(A, D)**, unlabeled cells stained with anti-CD34 **(B)** or anti-CD45 **(E)**, and CS-ATM DM Green-labeled cells stained with anti-CD34 **(C)** or anti-CD45 **(F)**.

Table 2. Characterization of CS-ATM DM Green uptake in final stromal vascular fraction cell product

CS-1000-positive cells	Average ± SD, %
All cells	37.1 ± 28.1
CD45+	47.8 ± 18.5
CD34+	87.0 ± 13.5
CD31+	92.7 ± 5.0
CD45−/CD31−/CD34−	16.4 ± 22.3

Data are presented for $n = 4$ independent experiments.

retained in cells and 9.4% was released into the supernatant (Fig. 4). In sharp contrast, cells exposed to staurosporine or freeze/thaw cycles contained only 3.9% and 6.0% of the fluorine content of untreated cell cultures, respectively.

MRI Detection of ^{19}F-Labeled Cells

To determine the feasibility of clinical MRI detection at 3T, we injected three different amounts of CS-1000-labeled SVF cells at two different depths (5 or 10 mm below the surface of the implant) in a silicone breast phantom (Fig. 5). ^{1}H MRI coronal and sagittal views confirmed the accuracy of all injection sites as seen from the optical diagram (Fig. 5Ai–Aiv). However, on ^{19}F MRI, only the 2-million cell sample injected 5 mm below the implant surface generated enough signal to be visible (Fig. 5B). None of the cells

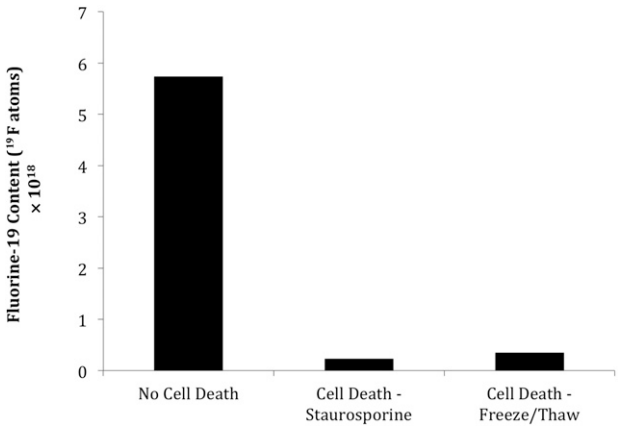

Figure 4. Fate of ^{19}F after induction of cell death. ^{19}F-labeled cells were exposed to staurosporine or freeze/thaw cycles to induce apoptotic and necrotic cell death, respectively, with untreated cells as the control. After 4 days, dead cells and cell debris were harvested by centrifugation, washed, and analyzed by nuclear magnetic resonance (NMR) for ^{19}F content. Shown is the total ^{19}F content for three independent runs, which were pooled to create sufficient signal for NMR detection.

injected at 10 mm below the surface were detected. An overlay of the cellular fluorine signal and the optical diagram confirmed the cells as having a ^{19}F source (Fig. 5C).

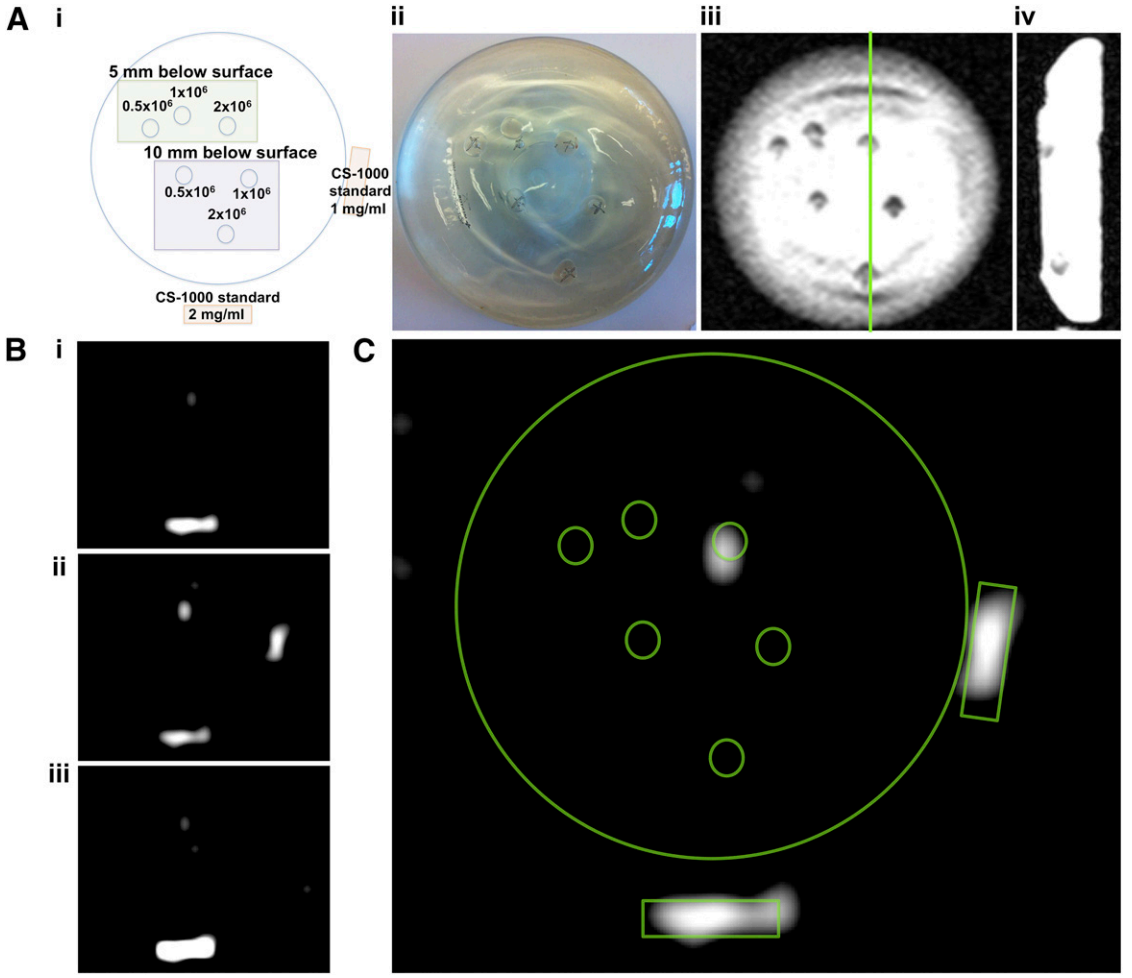

Figure 5. ^{19}F 3-Tesla magnetic resonance imaging (MRI) of labeled stromal vascular fraction (SVF) cells in a silicone breast phantom. **(Ai):** Diagram outlines the six cell injection variables (0.5, 1.0, and 2.0 $\times$ 10^6 cells injected at either 5- or 10-mm depth) and CS-1000 standards. **(Aii):** An optical image of the final injected breast implant phantom. Coronal **(Aiii)** and sagittal **(Aiv)** ^{1}H MR images of the phantom show nonspecific contrast from injection sites. **(Bi–Biii):** Sequential ^{19}F MR images of the phantom show MRI signal only for 2.0 $\times$ 10^6 cells injected at a 5-mm depth. **(C):** This was confirmed by overlaying the cell and standard diagram on the slice from **(Bii)**.

Discussion

Adipose tissue is emerging as a favorable site for therapeutic (stem) cell harvesting, because relatively large volumes with high progenitor cell yields can be obtained quickly and without significant morbidity compared with blood- and bone marrow-derived stem cells [28]. Several tissue-processing systems are currently available to address point-of-care delivery needs. A comparison of four commercially available systems found considerable variation in cell yield and residual enzyme content, among other factors, with the nearly fully automated Celution from Cytori Therapeutics, Inc. (San Diego, CA, http://www.cytori.com) leading the outcome of most assessment parameters [29]. Although we did not perform a direct comparison, the GID SVF-1 results from the present study suggest parity with the cell yields that can be obtained with the Celution, despite the lack of an RBC removal step in the Celution protocol. Higher yields have been reported with GID SVF-1 [26] but that protocol lacked both postdigest washes and an RBC removal step, both of which result in significant cell loss. Additional washings are critical, not only to remove residual enzyme that can potentially damage soft tissue [29], but also to remove dead cells and debris that might initiate orpropagate cell death cascades.

We found a significant amount of cell death when we used LR to process SVF. Despite its previous use for harvesting SVF cells, LR itself has no buffer system, unlike the 10-mM phosphate-based buffer system in PBS. LR is an alkalizing solution, such that on administration, lactate is converted to bicarbonate in the presence of oxygen primarily by the liver with some metabolic contribution from kidneys [30]. Cell death has been previously reported for cells exposed to LR in vitro [31, 32]. The use of LR in the closed system for digestion of adipose tissue might present unexpected challenges, potentially contributing to the inconsistent results. We observed insufficient mixing when processing adipose volumes close to the maximum capacity, which might prevent sufficient oxygenation and inhibit lactate metabolism. In addition, the pH of LR as reported from the manufacturer is 6.5, with an expected range of 6.0–7.5 as the final pH, if not adjusted. Exposure to a lower suboptimal pH value has the potential to damage isolated SVF cells. Finally, it is not clear whether adipose tissue can metabolize lactate quickly enough to provide a sufficient bicarbonate buffer for cells, especially if the starting pH is low. Such variations in the harvesting and processing conditions could lead to undesirable irregularities in the final cell product. Thus, despite the ubiquitous availability of LR in surgical settings, it is not a

good choice for optimal cell survival and preservation. In contrast, PBS has also been used for preclinical harvesting of SVF and for processing other cells for clinical use [33, 34] and has arguably better properties for this purpose, as demonstrated by our cell death profiles and previous reports [31]. The composition of cells obtained with our harvest and labeling protocol are in agreement with a joint position statement from the International Federation for Adipose Therapeutics and Science and the International Society for Cellular Therapy [35], which provides a guideline for the definition of SVF cells.

The decision to include an RBC lysis step was predicated on the large number of residual RBCs in the final cell product. Although RBCs do not take up CS-1000 [36], the presence of large numbers of RBCs complicates labeling and analysis, especially because less than one half of the overall SVF cells are labeled. RBC removal is routine in blood-derived stem cells [28] and frequently included in bone marrow-derived stem cells [37], in particular for cellular imaging studies [38]. With one exception, previously published SVF trials did not track cells after administration, and no RBC removal was included in the protocols [5, 33]. For the sole clinical study that had included a cell-tracking component, the SVF cells were treated with an RBC lysis buffer before labeling with the radiotracer [14]. Despite slight differences previously observed in SVF cells treated with lysis buffer or gradient centrifugation [39], we found no differences in CS-1000 labeling; hence, we selected the lysis buffer instead of gradient density centrifugation owing to its short completion time and lower risk for error.

The clinical importance of MRI cell tracking was demonstrated in a first-in-human study in which SPIO-labeled cells were injected to lymph nodes under ultrasound guidance. It was a major surprise when MRI demonstrated that cells were delivered incorrectly (e.g., injected into the surrounding fat tissue) in 50% of the cases [12]. Although the same group had performed ^{111}In-labeled cell studies using the same clinical scenario, owing to the lack of anatomical information on radionuclide scans, the error in delivery localization had not been realized previously [40]. Regardless, failure to deliver therapeutic cells to the required target tissue could contribute to treatment failure. Although the injured tissue of patients with RIF for the proposed study presents an arguably easier target, it remains unknown how long cells survive and whether cells migrate to injured tissue or remain at the injection site. Such information will help to expand successful use of SVF and other cell therapies. With the discontinuation of clinical-grade SPIO approved by the FDA for MRI studies, fluorinated reagents, such as CS-1000, now offer an alternative reagent for noninvasive cell tracking. A recent position statement identified highly desirable SVF cells such as CD45−/CD235a−/CD31−/CD34+, but these constitute only 15%–30% of SVF cells [35]. Other major cell types included CD45+ hematopoietic lineage and CD31+ endothelial lineage cells, and such complexity of subpopulations might influence ^{19}F-labeling efforts. Therefore, labeling heterogeneous SVF cells necessitates examination of subpopulations to either confirm homogenous uptake or identify which cells become labeled. In contrast to purified adipose-derived stem cells or mesenchymal stem cells (MSCs), SVF cells are a heterogeneous population of stem cells and other cells. SVF contains adult MSCs, preadipocytes (lineage-committed stem cells), endothelial cells, fibroblasts, pericytes, and inflammatory cells, such as macrophages, neutrophils, mast cells, and dendritic cells [41]. Previous ^{19}F ex vivo-labeling studies have only reported uptake in relatively uniform cultures such as dendritic [19], hematopoietic [42], or mesenchymal [43] stem cells. However, differential uptake was demonstrated in different populations of cells of whole blood after intravenous delivery of ^{19}F emulsions, in which signal was observed in white, but not red, blood cells [36]. The importance of more detailed assays for evaluating uptake in heterogeneous cultures is particularly emphasized with our new finding that CS-1000 selectively labels certain subpopulations. During the short 4-hour incubation period used in this protocol, CS-ATM DM Green preferentially labeled CD34+ cells. In contrast, fewer than one half of the CD45+ cells were CS-ATM DM Green labeled, with a significant unlabeled subpopulation of CD45+ cells. The reasons for preferential uptake are unclear but might be related to the increased phagocytosis of stem cells [17, 44] and some hematopoietic cells. It is possible that a more prolonged incubation period with CS-1000/CS-ATM DM Green would allow more homogeneous label uptake. However, the dynamic nature of SVF cells present challenges: prolonged incubation periods allow plastic adherent subpopulations to attach and nonadherent suspension subpopulations die. Although culturing cells before labeling would likely allow more uniform labeling, freshly harvested SVF cells might offer superior efficacy compared with cultured cells [45], and allow the performance of same-day surgical procedures. Furthermore, the use of uncultured SVF cells circumvents both the considerable expense of ex vivo expansion under current Good Manufacturing Process (cGMP) and the detrimental effects from aggressive expansion, hypothesized to be responsible for the lack of therapeutic effects in some trials [46]. Ultimately, the heterogeneous pattern of labeling is not detrimental for tracking SVF cells, because progenitor CD34+ cells are believed to be one of the main effectors of cell therapy.

In addition to the benefits of hotspot imaging, CS-1000 might also offer discrimination between live and dead cells. Dual-labeled MSCs showed a decline in signal from CS-1000 but not from SPIO over time [43]. Other studies have reported retention of SPIO particles after cell death [22, 47], but no studies have specifically investigated whether dead cells retain or lose the ^{19}F label. The loss of ^{19}F after cell death suggests that CS-1000 is only retained in live cells.

With ^{19}F MRI, we were able to detect a threshold of approximately 2×10^6 CS-1000-labeled SVF cells injected at a depth of 5 mm under the breast phantom surface. Through liposuction, it is possible to extract large volumes of fat with minimal morbidity compared with the procedure for bone marrow aspiration, which is uncomfortable and cannot yield large tissue volumes [48]. Lipoaspiration of volumes as small as 200 cm^3 can deliver a therapeutic dose of SVF cells (with $5–7 \times 10^5$ SVF cells per cubic centimeter of fat) well in excess of 100 million cells within a single operative session of less than a few hours [49]. Because $1–2 \times 10^8$ million SVF cells is the current recommended dose for RIF therapy in breast cancer [50], our threshold of cell detection was approximately two orders of magnitude lower than what would be needed for their detection in patients for a given distance (tissue depth) from the surface coil. Additional improvements in sensitivity might be obtained by using dedicated volume coils, longer acquisition times, and/or the use of higher field clinical scanners.

Conclusion

CS-1000-labeled SVF cells can be detected with ^{19}F MRI on a 3T clinical scanner with sufficient sensitivity to allow for clinical studies. Preferential labeling of CD34$^+$ progenitor cells underscores the heterogeneity of SVF cells and the importance of investigating mixed cell subpopulations, given the increased preference to use uncultured cells in regenerative medicine.

Acknowledgments

This study was funded by the Maryland Stem Cell Research Foundation (Grant MSCRFE-0040). We thank Dr. William Cimino, Dr. William Futrell, and the GID Group for their assistance with protocol development.

Author Contributions

L.C.R.: conception and design, collection and/or assembly of data, data analysis and interpretation, manuscript writing; D.K.K., G.W., A.B.-S., and D.L.K.: collection and/or assembly of data; B.M.H. and C.F.O: provision of study material or patients, data analysis and interpretation; R.L.R.: conception and design, provision of study material or patients, final approval of manuscript; J.W.M.B.: conception and design, data analysis and interpretation, manuscript writing, final approval of manuscript.

Disclosure of Potential Conflicts of Interest

B.M.H. is an employee of Celsense, Inc., and has stock options with Celsense, Inc. C.F.O. is an employee of Celsense, Inc., a shareholder of Celsense, Inc., and an officer and director of Celsense, Inc. D.L.K. has compensated grant support. The other authors indicated no potential conflicts of interest.

References

1 Hopwood P, Haviland JS, Sumo G et al. Comparison of patient-reported breast, arm, and shoulder symptoms and body image after radiotherapy for early breast cancer: 5-Year follow-up in the randomised Standardisation of Breast Radiotherapy (START) trials. Lancet Oncol 2010;11:231–240.

2 Bentzen SM, Trotti A. Evaluation of early and late toxicities in chemoradiation trials. J Clin Oncol 2007;25:4096–4103.

3 Constine LS, Friedman D, Morris M et al. Late effects of cancer treatment on normal tissues. In: Halperin EC, Brady LW, eds. Perez and Brady's Principles and Practice of Radiation Oncology, 4th edPhiladelphia: Lippincott Williams & Wilkins; 2004320–355.

4 Gentile P, Orlandi A, Scioli MG et al. Concise review: Adipose-derived stromal vascular fraction cells and platelet-rich plasma: Basic and clinical implications for tissue engineering therapies in regenerative surgery. Stem Cells Translational Medicine 2012;1: 230–236.

5 Gentile P, Orlandi A, Scioli MG et al. A comparative translational study: The combined use of enhanced stromal vascular fraction and platelet-rich plasma improves fat grafting maintenance in breast reconstruction. Stem Cells Translational Medicine 2012; 1:341–351.

6 Yoshimura K, Sato K, Aoi N et al. Cell-assisted lipotransfer for facial lipoatrophy: Efficacy of clinical use of adipose-derived stem cells. Dermatol Surg 2008;34:1178–1185.

7 Rigotti G, Marchi A, Galie M et al. Clinical treatment of radiotherapy tissue damage by lipoaspirate transplant: A healing process mediated by adipose-derived adult stem cells. Plast Reconstr Surg 2007;119: 1409–1423.

8 Yoshimura K, Sato K, Aoi N et al. Cell-assisted lipotransfer for cosmetic breast augmentation: Supportive use of adipose-derived stem/stromal cells. Aesthet Plast Surg 2008; 32:48–56.

9 Rigotti G, Marchi A, Stringhini P et al. Determining the oncological risk of autologous lipoaspirate grafting for post-mastectomy breast reconstruction. Aesthetic Plast Surg 2010;34:475–480.

10 Yoshimura K. Progenitor enriched adipose tissue transplantation as rescue for breast implant complications. Breast J 2010; 16:169–175.

11 Galipeau J. The mesenchymal stromal cells dilemma—Does a negative phase III trial of random donor mesenchymal stromal cells in steroid-resistant graft-versus-host disease represent a death knell or a bump in the road? Cytotherapy 2013;15:2–8.

12 de Vries IJ, Lesterhuis WJ, Barentsz JO et al. Magnetic resonance tracking of dendritic cells in melanoma patients for monitoring of cellular therapy. Nat Biotechnol 2005;23:1407–1413.

13 Schächinger V, Aicher A, Döbert N et al. Pilot trial on determinants of progenitor cell recruitment to the infarcted human myocardium. Circulation 2008;118:1425–1432.

14 Tzouvelekis A, Paspaliaris V, Koliakos G et al. A prospective, non-randomized, no placebo-controlled, phase Ib clinical trial to study the safety of the adipose derived stromal cells-stromal vascular fraction in idiopathic pulmonary fibrosis. J Transl Med 2013; 11:171.

15 Bulte JW. In vivo MRI cell tracking: Clinical studies. AJR Am J Roentgenol 2009;193: 314–325.

16 Khurana A, Nejadnik H, Chapelin F et al. Ferumoxytol: A new, clinically applicable label for stem-cell tracking in arthritic joints with MRI. Nanomedicine (Lond) 2013;8:1969–1983.

17 Bulte JW. Science to practice: Can stem cells be labeled inside the body instead of outside? Radiology 2013;269:1–3.

18 Gutova M, Frank JA, D'Apuzzo M et al. Magnetic resonance imaging tracking of ferumoxytol-labeled human neural stem cells: Studies leading to clinical use. Stem Cells Translational Medicine 2013;2:766–775.

19 Ahrens ET, Flores R, Xu H et al. In vivo imaging platform for tracking immunotherapeutic cells. Nat Biotechnol 2005;23:983–987.

20 Ruiz-Cabello J, Walczak P, Kedziorek DA et al. In vivo "hot spot" MR imaging of neural stem cells using fluorinated nanoparticles. Magn Reson Med 2008;60:1506–1511.

21 Barnett BP, Ruiz-Cabello J, Hota P et al. Use of perfluorocarbon nanoparticles for non-invasive multimodal cell tracking of human pancreatic islets. Contrast Media Mol Imaging 2011;6:251–259.

22 Gaudet JM, Ribot EJ, Chen Y et al. Tracking the fate of stem cell implants with fluorine-19 MRI. PLoS One 2015;10:e0118544.

23 Bulte JW. Hot spot MRI emerges from the background. Nat Biotechnol 2005;23:945–946.

24 Ahrens ET, Helfer BM, O'Hanlon CF et al. Clinical cell therapy imaging using a perfluorocarbon tracer and fluorine-19 MRI. Magn Reson Med 2014;72:1696–1701.

25 Verma VK, Beevi SS, Tabassum A et al. In vitro assessment of cytotoxicity and labeling efficiency of 99mTc-HMPAO with stromal vascular fraction of adipose tissue. Nucl Med Biol 2014;41:744–748.

26 Dos-Anjos Vilaboa S, Navarro-Palou M, Llull R. Age influence on stromal vascular fraction cell yield obtained from human lipoaspirates. Cytotherapy 2014;16:1092–1097.

27 Takeichi M. Cadherin cell adhesion receptors as a morphogenetic regulator. Science 1991;251:1451–1455.

28 Hamadani M. Autologous hematopoietic cell transplantation: An update for clinicians. Ann Med 2014;46:619–632.

29 Aronowitz JA, Ellenhorn JD. Adipose stromal vascular fraction isolation: A head-to-head comparison of four commercial cell separation systems. Plast Reconstr Surg 2013;132: 932e–939e.

30 Marik PE, Bellomo R. Lactate clearance as a target of therapy in sepsis: A flawed paradigm. OA Critical Care 2013;1:3.

31 Simpkins CO, Ekshyyan V, Snyder B. Histidine inhibits the degradation of cells suspended in Ringer's lactate. J Trauma 2007;63:565–572.

32 Simpkins CO, Little D, Brenner A et al. Heterogeneity in the effect of albumin and other resuscitation fluids on intracellular oxygen free radical production. J Trauma 2004; 56:548–558.

33 Kølle SF, Fischer-Nielsen A, Mathiasen AB et al. Enrichment of autologous fat grafts with ex-vivo expanded adipose tissue-derived stem cells for graft survival: A randomised placebo-controlled trial. Lancet 2013;382: 1113–1120.

34 Trojahn Kølle SF, Oliveri RS, Glovinski PV et al. Pooled human platelet lysate versus fetal bovine serum—Investigating the proliferation rate, chromosome stability and angiogenic potential of human adipose tissue-derived stem cells intended for clinical use. Cytotherapy 2013;15:1086–1097.

35 Bourin P, Bunnell BA, Casteilla L et al. Stromal cells from the adipose tissue-derived stromal vascular fraction and culture expanded adipose tissue-derived stromal/stem cells: A joint statement of the International Federation for Adipose Therapeutics and Science (IFATS) and the International Society for Cellular Therapy (ISCT). Cytotherapy 2013; 15:641–648.

36 Ebner B, Behm P, Jacoby C et al. Early assessment of pulmonary inflammation by ^{19}F MRI in vivo. Circ Cardiovasc Imaging 2010; 3:202–210.

37 Haack-Sørensen M, Friis T, Mathiasen AB et al. Direct intramyocardial mesenchymal stromal cell injections in patients with severe refractory angina: One-year follow-up. Cell Transplant 2013;22:521–528.

38 Musialek P, Tekieli L, Kostkiewicz M et al. Infarct size determines myocardial uptake of CD34+ cells in the peri-infarct zone: results from a study of (99m)Tc-extametazime-labeled cell visualization integrated with cardiac magnetic resonance infarct imaging. Circ Cardiovasc Imaging 2013;6:320–328.

39 Najar M, Rodrigues RM, Buyl K et al. Proliferative and phenotypical characteristics of human adipose tissue-derived stem cells: Comparison of Ficoll gradient centrifugation and red blood cell lysis buffer treatment purification methods. Cytotherapy 2014;16:1220–1228.

40 De Vries IJ, Krooshoop DJ, Scharenborg NM et al. Effective migration of antigen-pulsed dendritic cells to lymph nodes in melanoma patients is determined by their maturation state. Cancer Res 2003;63:12–17.

41 Zimmerlin L, Donnenberg VS, Pfeifer ME et al. Stromal vascular progenitors in adult human adipose tissue. Cytometry A 2010;77: 22–30.

42 Helfer BM, Balducci A, Sadeghi Z et al. ^{19}F MRI tracer preserves in vitro and in vivo properties of hematopoietic stem cells. Cell Transplant 2013;22:87–97.

43 Ribot EJ, Gaudet JM, Chen Y et al. In vivo MR detection of fluorine-labeled human MSC using the bSSFP sequence. Int J Nanomedicine 2014;9:1731–1739.

44 Khurana A, Chapelin F, Beck G et al. Iron administration before stem cell harvest enables MR imaging tracking after transplantation. Radiology 2013;269:186–197.

45 Semon JA, Maness C, Zhang X et al. Comparison of human adult stem cells from adipose tissue and bone marrow in the treatment of experimental autoimmune encephalomyelitis. Stem Cell Res Ther 2014;5:2.

46 von Bahr L, Sundberg B, Lönnies L et al. Long-term complications, immunologic effects, and role of passage for outcome in mesenchymal stromal cell therapy. Biol Blood Marrow Transplant 2012;18:557–564.

47 Cianciaruso C, Pagani A, Martelli C et al. Cellular magnetic resonance with iron oxide nanoparticles: Long-term persistence of SPIO signal in the CNS after transplanted cell death. Nanomedicine (Lond) 2014;9:1457–1474.

48 Zhu M, Kohan E, Bradley J et al. The effect of age on osteogenic, adipogenic and proliferative potential of female adipose-derived stem cells. J Tissue Eng Regen Med 2009;3: 290–301.

49 Strem BM, Hicok KC, Zhu M et al. Multipotential differentiation of adipose tissue-derived stem cells. Keio J Med 2005;54: 132–141.

50 Pérez-Cano R, Vranckx JJ, Lasso JM et al. Prospective trial of adipose-derived regenerative cell (ADRC)-enriched fat grafting for partial mastectomy defects: The RESTORE-2 trial. Eur J Surg Oncol 2012;38:382–389.

